



Article

Non-Iterative, Unique, and Logical Formula-Based Technique to Determine Maximum Load Multiplier and Practical Load Multiplier for Both Transmission and Distribution Systems

Sharmistha Nandi ¹, Sriparna Roy Ghatak ¹, Parimal Acharjee ² and Fernando Lopes ^{3,*}

¹ School of Electrical Engineering, KIIT Deemed to be University, Bhubaneswar 751024, India; sharmisthanandi38@gmail.com (S.N.); sghatakfel@kiit.ac.in (S.R.G.)

² Electrical Engineering Department, National Institute of Technology, Durgapur 713209, India; parimal.acharjee@ee.nitdgp.ac.in

³ National Laboratory of Energy and Geology, 1649-038 Lisbon, Portugal

* Correspondence: fernando.lopes@lneg.pt

Abstract: In recent days, due to the increasing number of electric vehicle charging stations (EVCSs) and additional power consumption by domestic, commercial, and industrial consumers, the overall power system performance suffers, which further degrades voltage profile, reduces stability, increases losses, and may also create a voltage collapse problem. Therefore, it is crucial to predetermine a maximum loadability limit for voltage collapse analysis and a practical allowable extra load for safe and secure operation, keeping the bus voltage within the security limits. To mitigate the problems, unique and innovative formulae such as the maximum load multiplier (MLM) and practical load multiplier (PLM) have been developed to consider line resistance. The determination of actual permissible extra load for a bus enables quick assessment of bus-wise suitable capacities and the number of EVs that can be charged simultaneously in the charging station. The planning engineers can easily settle on the extra load demand by domestic, commercial, and industrial consumers, while maintaining the voltage security constraint. The proposed technique is simple, non-iterative, computationally inexpensive, and applicable to both transmission and distribution systems. The proposed work is tested on a 57-bus transmission system and 69-bus radial distribution system, and the obtained results from the developed formulae are verified by comparing with conventional iterative methods.

Keywords: maximum load multiplier; practical load multiplier; non-iterative unique logical formula; voltage limit; transmission and distribution systems



Citation: Nandi, S.; Ghatak, S.R.; Acharjee, P.; Lopes, F. Non-Iterative, Unique, and Logical Formula-Based Technique to Determine Maximum Load Multiplier and Practical Load Multiplier for Both Transmission and Distribution Systems. *Energies* **2023**, *16*, 4724. <https://doi.org/10.3390/en16124724>

Academic Editors: Byoung Kuk Lee and Abu-Siada Ahmed

Received: 10 April 2023

Revised: 9 June 2023

Accepted: 13 June 2023

Published: 15 June 2023



Copyright: © 2023 by the authors. Licensee MDPI, Basel, Switzerland. This article is an open access article distributed under the terms and conditions of the Creative Commons Attribution (CC BY) license (<https://creativecommons.org/licenses/by/4.0/>).

1. Introduction

The use of air conditioners, induction heaters, washing machines, microwave ovens, mixers, computers, and laptops is rapidly expanding as individuals strive to lead a more luxurious lifestyle [1]. This surge in demand is not limited to domestic settings; industrial and commercial sectors are also experiencing a continuous increase in load demand. Consequently, it is essential to accurately assess power consumption to ensure the secure and stable operation of the power system [2]. Furthermore, the rise of electric vehicles (EVs) has revolutionized the transportation sector by reducing environmental pollution through the use of electricity instead of fossil fuels [3,4]. As the demand for EVs continues to soar, the number of charging stations connected to buses has also grown rapidly [5–9]. Consequently, there has been a sharp increase in power demand, which can potentially lead to voltage limit violations or voltage collapse. To mitigate these risks, two types of maximum additional loads for a bus are of utmost importance to determine. Using MLM, the maximum load margin or maximum loadability limit can be identified to avoid voltage collapse. Using PLM, the practical maximum allowable extra load for a bus can be

evaluated for safe and secure power system operation, as the voltage should be within the security limits for practical operation.

To analyze voltage collapse and to know the load margin, the MLM is determined [10–14]. In this regard, the PV curve using Newton-Raphson Load Flow (NRLF) and continuation load flow (CLF) are commonly used [15–21]. In NRLF and CLF methods, both active and reactive loads are multiplied by the same multiplier to keep the power factor (pf) constant. Those methods are iterative methods and computationally expensive. Researchers and operating engineers of power systems also prefer simpler techniques and avoid programming complexity. In this context, the development of a non-iterative formula-based technique for the determination of maximum load limit would greatly assist in voltage stability analysis and enable easy identification of the voltage collapse point (VCP). To address this need, a unique and innovative formula has been devised for MLM calculation. This proposed technique is simple, non-iterative, and fast, offering a more efficient alternative. For verification of the results of the developed formula, voltage magnitude and execution time have been compared to well-known approaches, such as NRLF and CLF. In order to corroborate the formula, EVCSs are taken into consideration on load buses for both the 57-bus transmission system and the 69-bus radial distribution system (RDS), and the bus voltage result is evaluated to ensure that the security constraints are met.

From the voltage stability index (VSI), the weaker or weakest bus is identified [22–26]. Fast voltage stability index (FVSI) is commonly applied to find vulnerable buses as it takes less time [23,27,28]. It is also a non-iterative and formula-based technique. However, using FVSI, only the stability index or weaker buses can be determined, and MLM or load margin cannot be obtained. In addition, FVSI is not suitable for the distribution system as line resistance is neglected for calculation [29,30]. Thus, line resistance must be considered for developing MLM formulations to determine MLM or load margin. In [31], the authors have introduced a unique formula for calculating the maximum allowable active and reactive power for contingency analysis. In contrast, the proposed work involves calculating the maximum allowable load that can be added to a bus while ensuring system stability. In this regard, a new and effective formula for MLM determination is developed considering line resistance so that it can be applied in both transmission and distribution systems. Between these two formulae, one is considering the security constraints and other is not. In this paper, 57-bus as a transmission system [32,33] and 69-bus as RDS are [34,35] considered for result analysis.

Maximum loading capacity must be determined to avoid voltage instability or a voltage collapse problem. However, MLM cannot be used for practical power system operation since the voltage magnitude of the bus must be within security limitations in order to preserve power quality [36]. The allowable voltage range for the power system network is 0.9 to 1.1 p.u. [36,37]. Therefore, the practical allowable load which can be enhanced to a particular bus will be such that the voltage magnitude should not be less than 0.9 p.u. Considering the practical limits of voltage magnitudes of the buses, the PLM is formulated from MLM. Based on an extensive review of the existing literature, it is evident that a formula-based non-iterative PLM for both transmission and distribution systems was not developed at an early stage. However, this non-iterative approach is straightforward, efficient, and computationally inexpensive. By determining the PLM, it becomes possible to determine the maximum additional load that a bus can accommodate. For the different buses, different practical load margins will be attained. Hence, the most suitable capacity of an EV charging station can automatically be evaluated for the buses. Additionally, it enables the assessment of the number of EVs that can be charged simultaneously at the charging station. Furthermore, if the practical allowable extra load is known to the electricity company, it becomes feasible to promptly meet new load demands from residential, commercial, or industrial consumers in a justified and appropriate manner. The formulae of MLM and PLM are derived from the basic equation of line current, active power and reactive power flow, bus voltage, and phase angle of two buses of a single

machine infinite bus (SMIB) system. The results obtained from PLM are also checked and verified with conventional methods such as CLF and NRLF.

The major contributions of this paper are as follows:

1. A unique, innovative formula of MLM and PLM considering line resistance has been developed to evaluate the maximum load margin for voltage collapse and practical additional load for safe and secure power system operation, respectively, and the proposed formulae are applicable for both transmission and distribution systems.
2. The proposed technique is simple, non-iterative, and computationally inexpensive, and the obtained results from the developed formulae are vindicated by conventional iterative methods such as NRLF and CLF.
3. As the actual permissible extra load for a bus is determined using PLM, the bus-wise suitable capacities or ratings of EV charging stations can quickly be assessed. The planning engineers can also easily settle on the extra load demand by the domestic, commercial, and industrial consumers, keeping the voltage magnitude within the security limit.

2. Problem Formulation

A fast and non-iterative technique to determine MLM and PLM is important in the present power scenario. New and innovative formulations are developed to determine MLM and PLM, which are computationally inexpensive as well as non-iterative. It is also applicable to both transmission and distribution systems. To derive the formula, a simple two-bus system of the SMIB system is considered. In Figure 1, a two-bus simple network is shown, where line resistance is not neglected. Here, Bus-1 represents the generator bus and Bus-2 represents the load bus. The formula of MLM and PLM is derived from the fundamental equations between the two buses, such as active power and reactive power flow, the current flowing between the two buses, bus voltages, phase angle, etc.

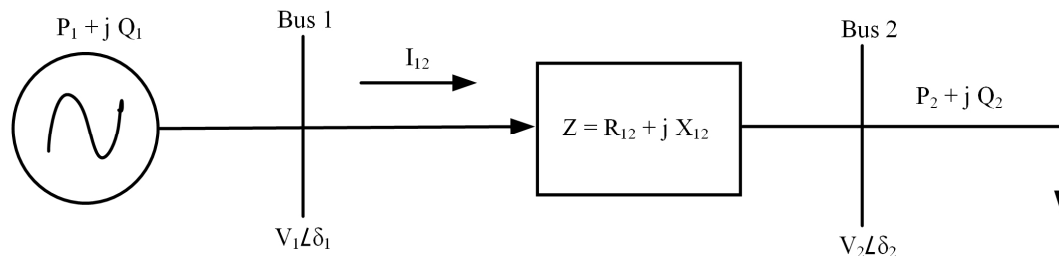


Figure 1. One-line diagram of power system network.

Where:

V_1 : A magnitude of the actual voltage at the sending end bus (SEB)

V_2 : A magnitude of the actual voltage at the receiving end bus (REB)

δ_1 : A phase angle of the voltage at the SEB

δ_2 : A phase angle of the voltage at the REB

P_1 : Active power at the SEB

P_2 : Active power at the REB

Q_1 : Reactive power at the SEB

Q_2 : Reactive power at the REB

Z : Line impedance between bus 1 and bus 2

R_{12} : Line resistance between SEB and REB

X_{12} : Line reactance between SEB and REB

I_{12} : Line current between SEB and REB

Let,

$\delta = \delta_1 - \delta_2$: Phase angle difference between the SEB and REB

Considering both the resistance and reactance of the line, the MLM is formulated as

$$MLM = \frac{|V_1|^2}{2(P_2X_{12} - Q_2R_{12})^2} \left\{ \sqrt{[(P_2R_{12} + Q_2X_{12})^2 + (P_2X_{12} - Q_2R_{12})^2]} - (P_2R_{12} + Q_2X_{12}) \right\} \quad (1)$$

The detailed derivation is given in Appendix A.

Equation (1) is the general formula of MLM, and it is useful for voltage collapse or voltage instability analysis. From MLM, for the practical operation of a power system, the maximum permissible load that can be applied practically to a bus cannot be obtained. The maximum allowable load for which the bus voltage will not violate the voltage limits is essential to determine safe and secure operation. The voltage of REB should be in the range of 0.9 p.u. to 1.1 p.u. [36,37]. However, by using (1), the bus voltage can decrease below 0.9 p.u., which is not acceptable for practical power system operation. Therefore, considering the practical limitations, the receiving end voltage should remain at 0.9 p.u. after the maximum allowable load enhancement. The generator bus voltage or SEB voltage is kept fixed. Considering the practical constraints, PLM is determined as follows:

$$PLM = \frac{\sqrt{\left\{ 4 * (0.9)^4 * (P_2R_{12} + Q_2X_{12})^2 \right\} - 4 * \left\{ (P_2R_{12} + Q_2X_{12})^2 + (P_2X_{12} - Q_2R_{12})^2 \right\} * \left\{ (0.9)^4 - |V_1|^2 * (0.9)^2 \right\}}}{2 * \left\{ (P_2R_{12} + Q_2X_{12})^2 + (P_2X_{12} - Q_2R_{12})^2 \right\}} - \frac{(0.9)^2 * 2(P_2R_{12} + Q_2X_{12})}{2 * \left\{ (P_2R_{12} + Q_2X_{12})^2 + (P_2X_{12} - Q_2R_{12})^2 \right\}} \quad (2)$$

From PLM, for the REB the actual additional load or practical load margin that can be enhanced while keeping the voltage magnitude in the security limits is obtained easily. It will be very helpful for the planning engineers to take a firm decision on the new load demand by the domestic/commercial/industrial consumers. Nowadays, EV charging stations are being installed worldwide. If the practical load margin is known for all buses, a suitable location and appropriate capacity of an EV charging station can also be determined.

3. Procedure

The formula used to calculate the MLM is employed in power systems to ensure the stability of the system. This formula is derived from (1). In this context, the bus at which MLM is calculated is referred to as the REB, while the bus supplying power to the REB is known as the SEB. The evaluation involves analysing two types of test systems: transmission and distribution systems. For the transmission system, 57-bus, and for RDS, 69-bus, are considered. As NRLF and CLF are commonly employed to determine MLM, the results of the unique and logical formula are compared to the results of the NRLF and CLF approaches. The load at the REB is gradually increased in conventional techniques, and convergence is tested in each run. When divergence occurs, MLM is determined for the conventional iterative methods and compared with the proposed technique.

For the practical operation of the power system, PLM is required instead of MLM so that the bus voltage will remain within the acceptable limit, 0.9 p.u. From MLM, PLM is derived, keeping the sending end voltage unaltered, and it is calculated using (2). The load multiplier for which the REB or the load bus voltage is at 0.9 p.u. is called PLM. Following the calculation of the PLM value using the proposed formula, the REB load will be multiplied by the PLM for both the NRLF and CLF techniques, and the results will be checked. The voltage magnitude should also be equal to 0.9 p.u. for the conventional methods. Being iterative methods, both NRLF and CLF take more time to give the desired results, whereas the proposed unique method gives the output directly as it is a non-iterative, formula-based approach.

After obtaining PLM for a specific bus, the extra load that can be allowed without violating the security constraints is analysed. As the maximum permissible additional load is established, the maximum acceptable new load demand or the suitable capacity of an EV charging station can be simply figured out. To carry out the load flow analysis,

MATLAB-9.8 (R2020a) platform has been used. It was installed on a computer with an Intel i7 processor, 1.3 GHz clock speed and 8 GB RAM. A flow chart of the detailed procedure is given in Figure 2.

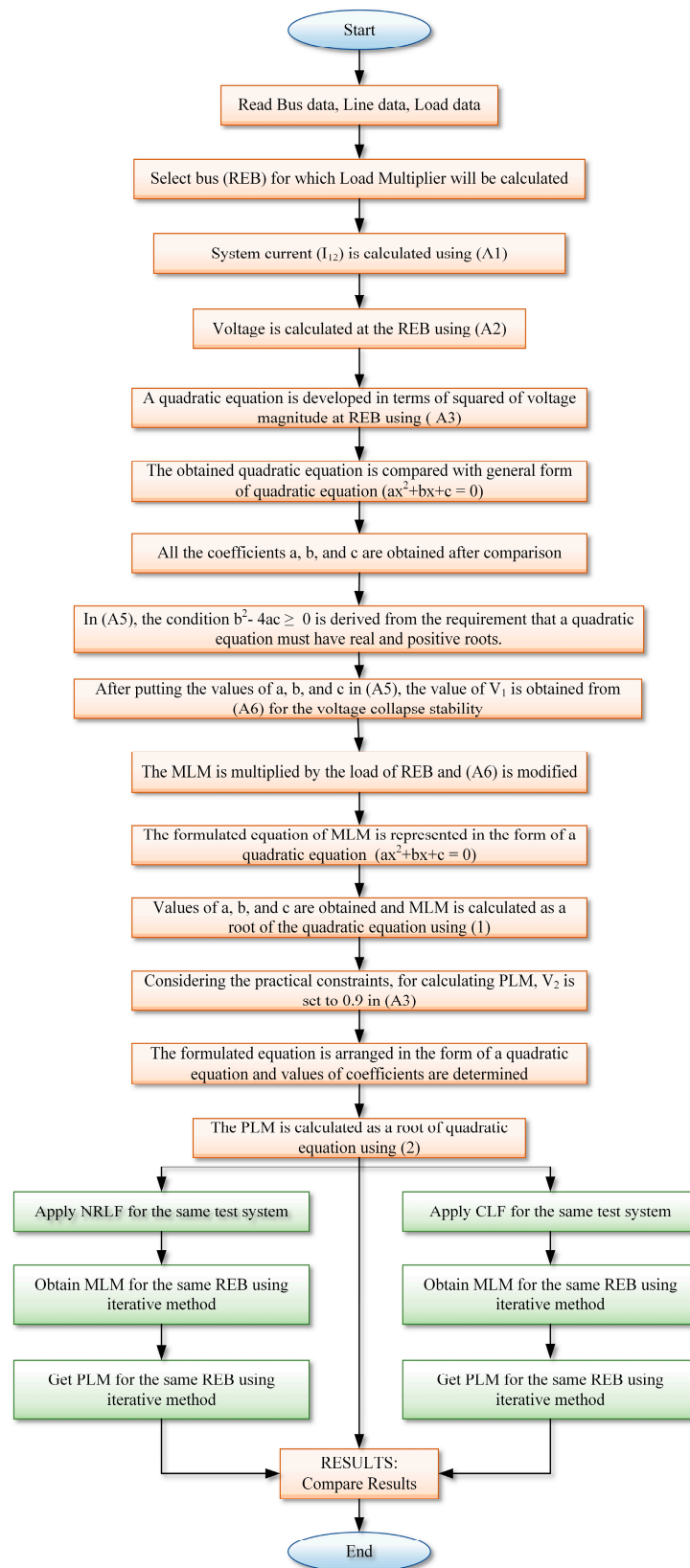


Figure 2. Flow chart of the procedure.

4. Result and Discussion

The developed formula of MLM and PLM is examined on both the interconnected transmission system, 57-bus, and RDS, 69-bus. The 57-bus system consists of 57 buses, 7 generators, 42 loads, and 63 transmission lines and has a base power of 100 MVA. The 69-bus system includes 69 buses and 73 lines and has a base voltage of 12.66 kV and a base power of 100 MVA.

For both the 57-bus transmission system and 69-bus RDS, 5 sets of buses are considered for finding MLM, PLM, and results analysis. The MLM of a bus is directly determined using (1) as the proposed approach is non-iterative and formula based. The MLM value is then reviewed by comparing it to the NRLF and CLF techniques. Comparison among NRLF, CLF, and the developed formula for MLM is shown in Table 1a,b for both 57-bus transmission systems and 69-bus RDS, respectively. From Table 1a,b, it can be observed that the value of MLM calculated using (1) is nearly the same as the value of MLM obtained from the NRLF and CLF methods. Though MLM provides the maximum loading limits or VCPs, it is crucial to refrain from operating the power system at such loads due to the significantly lower voltage magnitude, which falls below the lower voltage limit of the network. Hence, PLM is of utmost importance in knowing the practical loading limit for safe, secure power system operation.

Table 1. (a) Comparison among NRLF, CLF, and the developed formula for MLM for 57-Bus Transmission System. (b) Comparison among NRLF, CLF, and the developed formula for MLM for 69-Bus RDS.

| (a) | | | | | |
|---------|-----|-----|-------------------|---------------------------|--------------------------|
| Sl. No. | SEB | REB | MLM using formula | MLM using the NRLF method | MLM using the CLF method |
| 1 | 12 | 16 | 14.1780 | 14.2968 | 14.2969 |
| 2 | 19 | 20 | 19.7453 | 19.2339 | 19.7465 |
| 3 | 13 | 14 | 55.1172 | 56.9040 | 56.9041 |
| 4 | 41 | 42 | 8.0156 | 7.6986 | 8.0156 |
| 5 | 50 | 51 | 15.1357 | 16.2367 | 16.2369 |
| (b) | | | | | |
| Sl. No. | SEB | REB | MLM using formula | MLM using the NRLF method | MLM using the CLF method |
| 1 | 6 | 7 | 1850.9783 | 1851.1520 | 1851.1524 |
| 2 | 9 | 10 | 1254.8078 | 1254.8783 | 1254.8784 |
| 3 | 33 | 34 | 999.0980 | 998.9886 | 999.0981 |
| 4 | 48 | 49 | 123.3389 | 124.0974 | 124.8974 |
| 5 | 49 | 50 | 424.4114 | 423.8986 | 424.4114 |

Being a non-iterative method, the proposed formulae take significantly less time to give the results as compared to iterative methods. To prove the efficacy of the proposed method, a comparison of estimation of MLM for both 57-bus and 69-bus systems is performed using the MATLAB platform. For the NRLF method, the load is gradually incremented and the estimation time is calculated. The estimation time is computed in seconds (s). The comparison of estimation time between proposed and conventional methods is shown in Table 2a,b for both 57- and 69-bus systems, respectively. From Table 2a,b, it is observed that the computation time is significantly less in the case of the proposed method as compared to the conventional method, which proves the effectiveness of the proposed work.

Table 2. (a) Comparison of estimation time of MLM between the proposed method and the conventional method for a 57-bus transmission system. (b) Comparison of estimation time of MLM between the proposed method and the conventional method for a 69-bus RDS.

| (a) | | | | |
|---------|-----|-----|---|--|
| Sl. No. | SEB | REB | Estimation time for proposed method (s) | Estimation time for conventional method (NRLF) (s) |
| 1 | 12 | 16 | 0.000901 | 3.976398 |
| 2 | 19 | 20 | 0.000468 | 13.11175 |
| 3 | 13 | 14 | 0.001183 | 25.28018 |
| 4 | 41 | 42 | 0.000526 | 3.034557 |
| 5 | 50 | 51 | 0.000591 | 6.391836 |
| (b) | | | | |
| Sl. No. | SEB | REB | Estimation time for proposed method (s) | Estimation time for conventional method (NRLF) (s) |
| 1 | 6 | 7 | 0.000581 | 683.3324 |
| 2 | 9 | 10 | 0.000594 | 493.4006 |
| 3 | 33 | 34 | 0.000432 | 410.1328 |
| 4 | 48 | 49 | 0.000498 | 36.969733 |
| 5 | 49 | 50 | 0.000414 | 176.776818 |

Like MLM, the PLM is directly determined using (2) for 5 sets of buses of 57-bus and 69-bus test systems. The obtained PLM value is used in conventional iterative methods such as CLF and NRLF. When PLM is applied to the REB, the voltage magnitude of REB should also be 0.9 p.u. for the conventional methods. In the case of conventional methods, the PLM is multiplied by the REB and the results are verified. The PLM obtained from the developed formula, and the voltage magnitude of REB for the conventional methods, are given in Table 3a,b for 57-bus and 69-bus systems, respectively. From the tables, it is observed that the voltage magnitude of the REB is nearly 0.9 p.u. It confirms that the PLM value obtained from the developed formula and it can be used for the safe and secure operation of the power system.

Table 3. (a) Five sets of results of PLM for the 57-bus transmission system. (b) Five sets of results of PLM for 69-bus RDS.

| (a) | | | | |
|---------|------|-----|-------------------------------------|------------------------------|
| Sl. No. | SEB. | REB | PLM obtained from developed formula | Receiving end voltage (p.u.) |
| 1 | 12 | 16 | 6.99498 | 0.9031 |
| 2 | 19 | 20 | 5.74715 | 0.9082 |
| 3 | 13 | 14 | 18.49972 | 0.9015 |
| 4 | 41 | 42 | 2.99778 | 0.8981 |
| 5 | 50 | 51 | 8.02092 | 0.8994 |
| (b) | | | | |
| Sl. No. | SEB. | REB | PLM obtained from developed formula | Receiving end voltage (p.u.) |
| 1 | 6 | 7 | 616.4928 | 0.8997 |
| 2 | 9 | 10 | 372.218 | 0.8943 |
| 3 | 33 | 34 | 358.0564 | 0.9010 |
| 4 | 48 | 49 | 46.2458 | 0.8992 |
| 5 | 49 | 50 | 156.8488 | 0.9059 |

A graphical plot of voltage magnitude after applying PLM is shown below for both the 57- and 69-bus systems. After applying PLM at the 14th bus (REB), the voltage magnitude of the 57-bus transmission system is shown in Figure 3a. Similarly, the voltage magnitudes of a 69-bus RDS are given in Figure 3b when PLM is applied at the 34th bus (REB). From the two figures, it can be seen that the bus voltages of REB in both 57-bus and 69-bus test systems are the lowest and near 0.9 p.u. (i.e., 0.9015 p.u. and 0.9010 p.u., respectively), which is acceptable for practical operation. It is also observed that the bus voltage satisfies the lower voltage limit of the power system network.

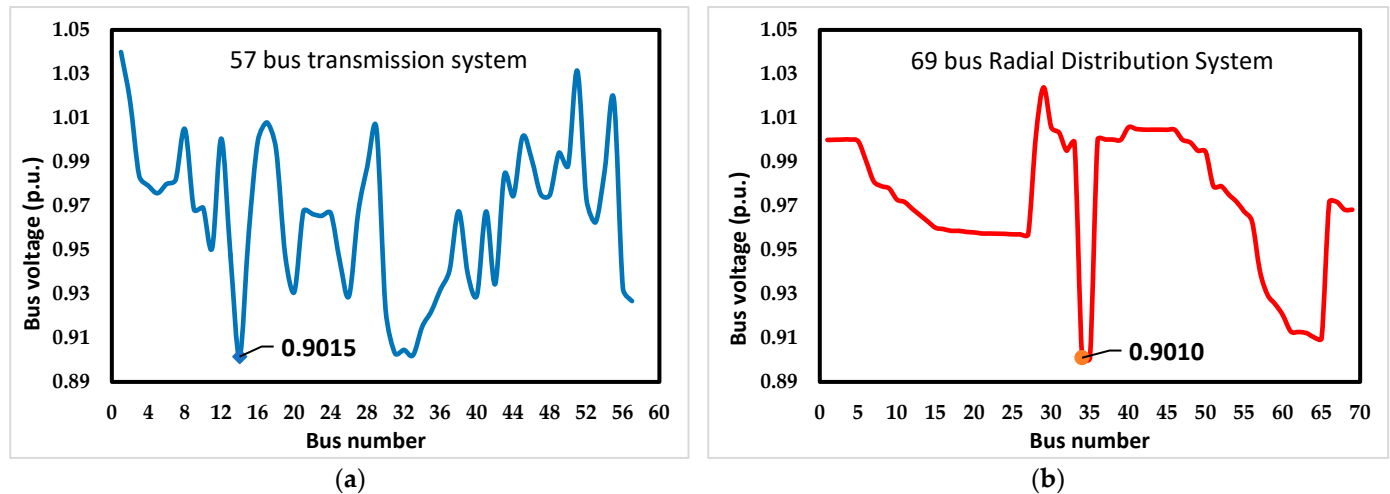
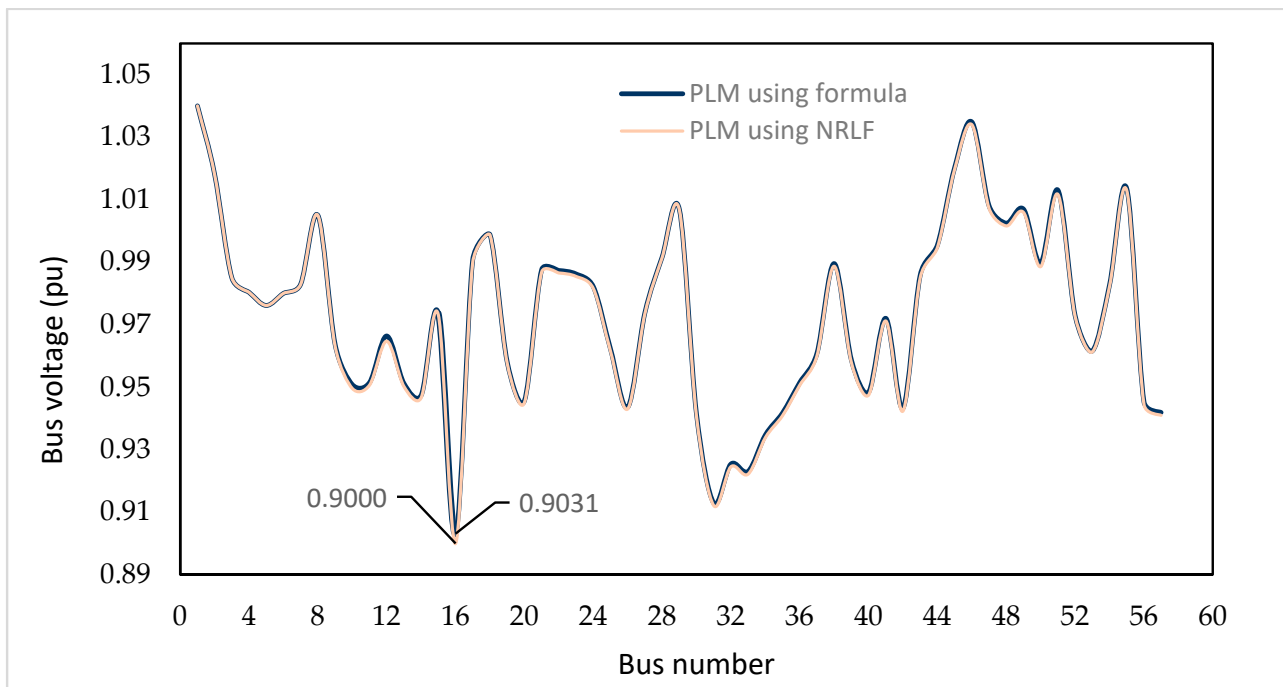
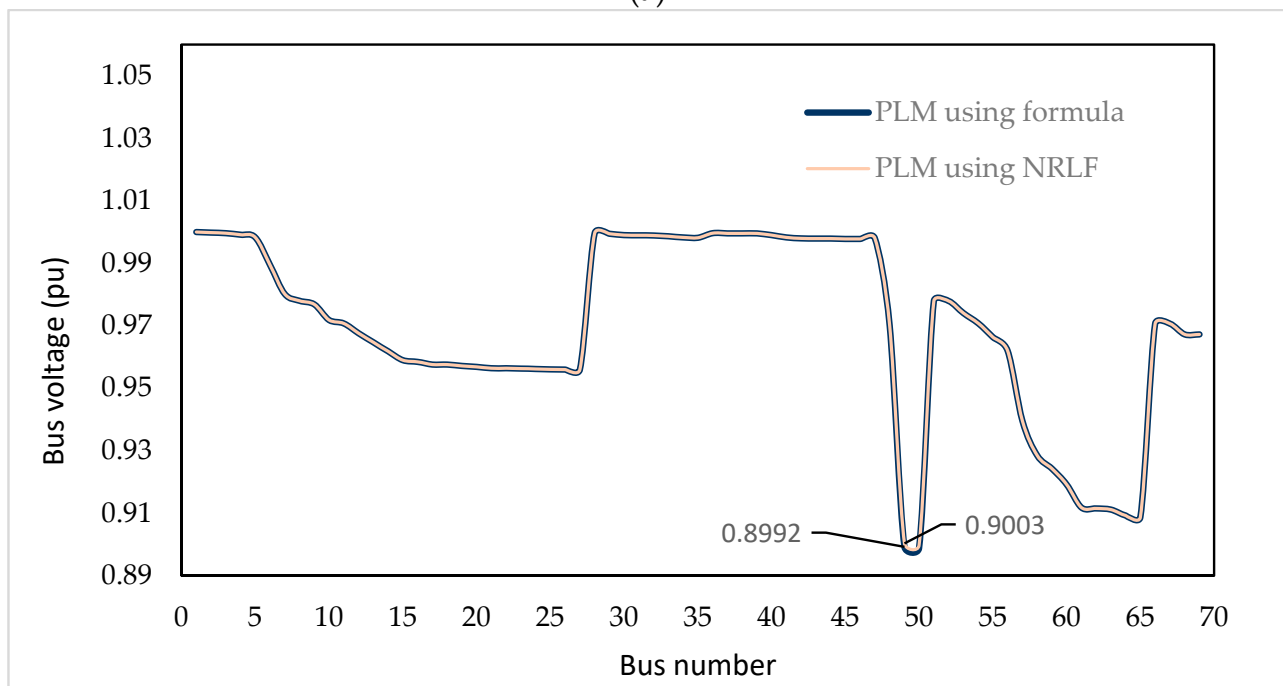


Figure 3. Sample result of voltage magnitude after applying PLM (a) For a 57-bus transmission system; (b) For a 69-bus RDS.

A comparison of voltage magnitude is performed after employing a load multiplier in both the proposed approach and the conventional method for both the 57-bus transmission system and the 69-bus RDS. The value of the load multiplier is calculated using the proposed method as well as using the NRLF method. The proposed load multiplier, obtained from both cases, is applied to the REB, and voltage is observed. Table 4a,b show the comparison of bus voltage magnitude after applying PLM in REB for both the 57-bus transmission system and the 69-bus RDS, respectively. From both tables, it is observed that the deviation in voltage at REB is very negligible. A graphical comparison of bus voltage is also shown below. The 16th bus in the 57-bus transmission system serves as an illustrative example to demonstrate the comparison of voltage magnitude between the conventional and proposed method for both PLM and MLM cases. These comparisons are presented in Figures 4a and 5a for the 57-bus system. Similarly, in the case of the 69-bus RDS, the 49th bus is selected as a sample example to showcase the voltage magnitude comparison between the conventional and proposed method for both PLM and MLM. Figures 4b and 5b display these comparisons for the 69-bus RDS. From Figure 4a,b, it is observed that there is a slight deviation in the voltage magnitude at the bus where the PLM is implemented, though the deviation is trivial/insignificant. However, the voltage magnitudes at the remaining buses (i.e., all other buses) are similar/matching for both the proposed method and the conventional method. Both the figures depict that the result attained using the proposed method is matching with the result obtained from the conventional iterative method (NRLF).



(a)



(b)

Figure 4. (a) Comparison of bus voltage (p.u.) between the proposed method and NRLF method after applying PLM at the 16th bus for the 57-bus transmission system. (b) Comparison of bus voltage (p.u.) between the proposed method and NRLF method after applying PLM at the 49th bus for the 69-bus RDS.

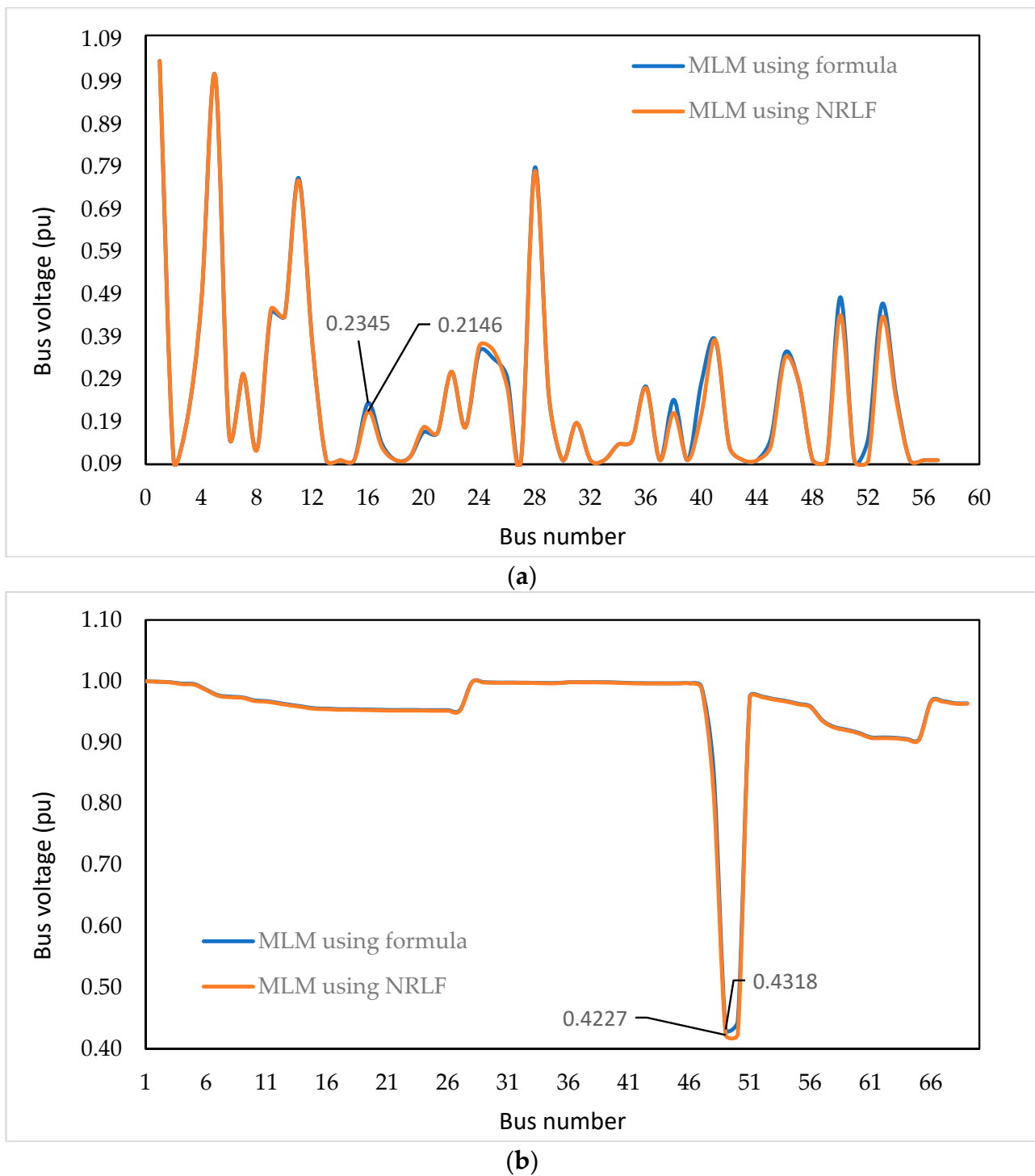


Figure 5. (a) Comparison of bus voltage (p.u.) between the proposed method and NRLF method after applying MLM at the 16th bus for a 57-bus transmission system. (b) Comparison of bus voltage (p.u.) between the proposed method and NRLF method after applying MLM at the 49th bus for a 69-bus RDS.

Table 4. (a) Comparison of voltage magnitude after applying PLM obtained from both the conventional and proposed method for a 57-bus system. (b) Comparison of voltage magnitude after applying PLM obtained from both the conventional and proposed method for a 69-bus system.

| (a) | | | |
|-----|-----|--|--|
| SEB | REB | Voltage at REB after applying PLM, obtained from formula | Voltage at REB after applying PLM, obtained using NRLF |
| 12 | 16 | 0.9031 | 0.9000 |
| 19 | 20 | 0.9082 | 0.9001 |
| 13 | 14 | 0.9015 | 0.9001 |
| 41 | 42 | 0.8981 | 0.8999 |
| 50 | 51 | 0.8994 | 0.9002 |
| (b) | | | |
| SEB | REB | Voltage at REB after applying PLM, obtained from formula | Voltage at REB after applying PLM, obtained using NRLF |
| 6 | 7 | 0.8997 | 0.9002 |
| 9 | 10 | 0.8943 | 0.8999 |
| 33 | 34 | 0.9010 | 0.9000 |
| 48 | 49 | 0.8992 | 0.9003 |
| 49 | 50 | 0.9059 | 0.9001 |

Figure 5a,b show the comparison of bus voltage between conventional and proposed methods when MLM is applied at REB for both the 57-bus transmission system and the 69-bus RDS, respectively. MLM is generally calculated to identify the VCP. Therefore, the voltage security constraint is not maintained in the case of MLM. From both the figures, it is observed that there is a slight variation in voltage, mostly where the MLM is applied in the proposed method as compared to the conventional method. On the other hand, voltage magnitude of the rest of the buses are almost the same in both the conventional and the proposed method. Therefore, it can be concluded that the proposed method for calculating the load multiplier gives the correct result.

The maximum additional load that can be added with the base load using MLM is given in Table 5a,b for the 57-bus System and the 69-bus RDS, respectively. From the tables, the maximum extra load for which the system will be at the VCP can be assessed for voltage stability analysis. The maximum practical allowable load obtained from PLM is shown in Table 6a,b for the 57-bus transmission system and the 69-bus RDS, respectively. The tables provide information on both active and reactive power loads that are permissible for ensuring safe and stable operation of the power system. From the tables, bus-wise practical permissible load enhancement is known, and it will be very useful for the permission of new connections and extra load demands by the existing consumers. In light of the recent installation of EV charging stations on buses, planning engineers can efficiently determine the most suitable buses and charging station capacities by referring to the acquired actual extra load data.

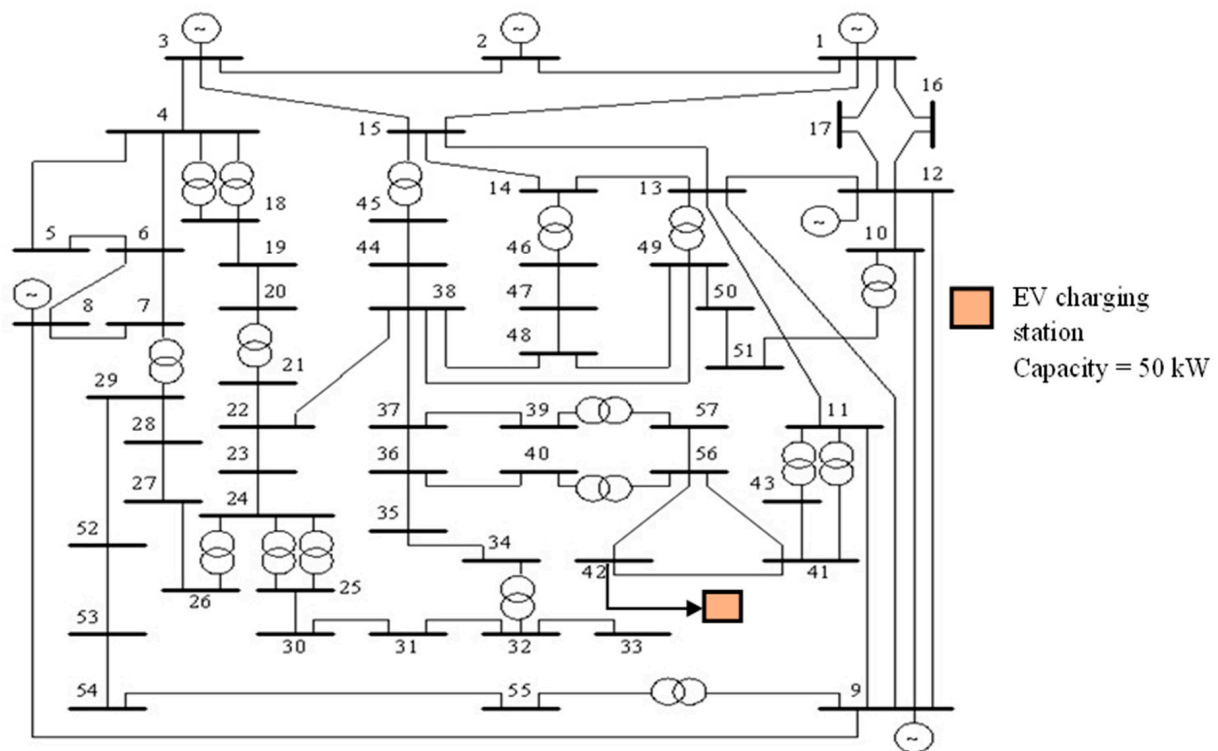
The proposed approach is rationalized by taking into account EVCS on load buses of the 57-bus transmission system and 69-bus RDS. The DC fast charging station with a capacity of 50 kW is considered to be placed on the load buses, and the bus voltage at the REB is shown in Table 7a,b for the 57-bus system and 69-bus RDS, respectively. From Table 7a,b it is observed that the voltage levels at the load bus remain within the prescribed security limits of 0.9 p.u. to 1.1 p.u. after the installation of the electric vehicle (EV) charging station. This outcome effectively fulfills the voltage constraints. Figure 6a shows a simplified figure of a 57-bus transmission system indicating the EV charging station at the 42nd load bus. Figure 6b represents a simplified figure of a 69-bus RDS indicating the EV charging station at the 34th load bus.

Table 5. (a) Maximum extra load that can be added with base load using MLM for a 57-bus system. (b) Maximum extra load that can be added with base load using MLM for a 69-bus system.

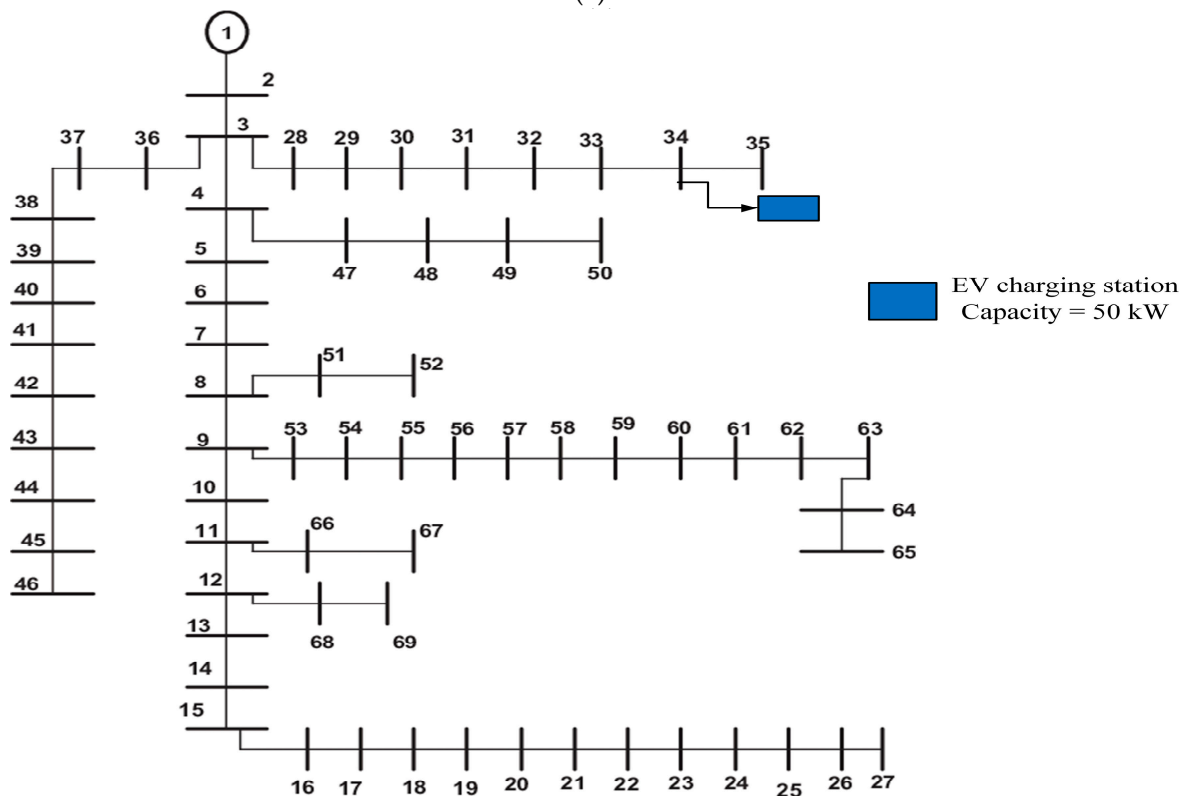
| (a) | | | | | | | | |
|---------|------|-----|-----------------|--------------|---|--------------|-----------------------|--------------|
| Sl. No. | SEB. | REB | Base load at RE | | Modified load after multiplying MLM at RE | | Additional load at RE | |
| | | | P_L (MW) | Q_L (MVar) | P_L (MW) | Q_L (MVar) | P_L (MW) | Q_L (MVar) |
| 1 | 12 | 16 | 43 | 3 | 678.5787 | 47.3427 | 635.5787 | 44.3427 |
| 2 | 19 | 20 | 2.3 | 1 | 45.4142 | 19.7453 | 43.1142 | 18.7453 |
| 3 | 13 | 14 | 10.5 | 5.3 | 578.7306 | 292.1212 | 568.2306 | 286.8212 |
| 4 | 41 | 42 | 7.1 | 4 | 56.9113 | 32.0627 | 49.8113 | 28.0627 |
| 5 | 50 | 51 | 18 | 5.3 | 218.4341 | 64.3167 | 200.4341 | 59.0167 |
| (b) | | | | | | | | |
| Sl. No. | SEB | REB | Base load at RE | | Modified load after multiplying MLM at RE | | Additional load at RE | |
| | | | P_L (MW) | Q_L (MVar) | P_L (MW) | Q_L (MVar) | P_L (MW) | Q_L (MVar) |
| 1 | 6 | 7 | 0.04 | 0.03 | 74.0332 | 55.5249 | 73.9932 | 55.4949 |
| 2 | 9 | 10 | 0.03 | 0.02 | 37.6202 | 25.0802 | 37.5902 | 37.6002 |
| 3 | 33 | 34 | 0.02 | 0.01 | 19.982 | 9.991 | 19.962 | 9.981 |
| 4 | 48 | 49 | 0.38 | 0.27 | 46.8688 | 33.3025 | 46.4888 | 33.0315 |
| 5 | 49 | 50 | 0.38 | 0.27 | 161.2763 | 114.5911 | 160.8963 | 114.3211 |

Table 6. (a) Maximum practical allowable load obtained from PLM for a 57-bus system. (b) Maximum practical allowable load obtained from PLM for a 69-bus RDS.

| (a) | | | | | | | | |
|---------|-----|-----|-----------------|--------------|---|--------------|-----------------------|--------------|
| Sl. No. | SEB | REB | Base load at RE | | Modified load after multiplying PLM at RE | | Additional load at RE | |
| | | | P_L (MW) | Q_L (MVar) | P_L (MW) | Q_L (MVar) | P_L (MW) | Q_L (MVar) |
| 1 | 12 | 16 | 43 | 3 | 300.7841 | 20.9849 | 257.7841 | 17.9849 |
| 2 | 19 | 20 | 2.3 | 1 | 13.2184 | 5.7471 | 10.9184 | 4.7471 |
| 3 | 13 | 14 | 10.5 | 5.3 | 194.2471 | 98.0485 | 183.7471 | 92.7485 |
| 4 | 41 | 42 | 7.1 | 4 | 21.2842 | 11.9911 | 14.1842 | 7.9911 |
| 5 | 50 | 51 | 18 | 5.3 | 144.3766 | 42.5109 | 126.3766 | 37.2109 |
| (b) | | | | | | | | |
| Sl. No. | SEB | REB | Base load at RE | | Modified load after multiplying PLM at RE | | Additional load at RE | |
| | | | P_L (MW) | Q_L (MVar) | P_L (MW) | Q_L (MVar) | P_L (MW) | Q_L (MVar) |
| 1 | 6 | 7 | 0.04 | 0.03 | 24.66 | 18.495 | 24.62 | 18.465 |
| 2 | 9 | 10 | 0.03 | 0.02 | 11.17 | 7.44 | 11.14 | 7.42 |
| 3 | 33 | 34 | 0.02 | 0.01 | 7.16 | 3.58 | 7.14 | 3.57 |
| 4 | 48 | 49 | 0.38 | 0.27 | 17.57 | 12.49 | 17.19 | 12.22 |
| 5 | 49 | 50 | 0.38 | 0.27 | 59.6 | 42.35 | 59.22 | 42.08 |



(a)



(b)

Figure 6. (a) A simplified figure of the 57-bus system after placing the charging station at the 42nd load bus. (b) A simplified figure of the 69-bus RDS after placing the charging station at the 34th load bus.

Table 7. (a) Voltages at REB after placing charging station on load bus for a 57-bus transmission system. (b) Voltages at REB after placing charging station on load bus for a 69-bus RDS.

| (a) | | | | | |
|---------|-----|-----|--|--|-------------------------------------|
| Sl. No. | SEB | REB | Base active power load at receiving end bus (MW) | Base reactive power load at receiving end bus (MVar) | Voltage at receiving end bus (p.u.) |
| 1 | 12 | 16 | 43 | 3 | 1.0134 |
| 2 | 19 | 20 | 2.3 | 1 | 0.9626 |
| 3 | 13 | 14 | 10.5 | 5.3 | 0.9681 |
| 4 | 41 | 42 | 7.1 | 4 | 0.9682 |
| 5 | 50 | 51 | 18 | 5.3 | 1.0520 |
| (b) | | | | | |
| Sl. No. | SEB | REB | Base active power load at receiving end bus (MW) | Base reactive power load at receiving end bus (MVar) | Voltage at receiving end bus (p.u.) |
| 1 | 6 | 7 | 0.04 | 0.03 | 0.9805 |
| 2 | 9 | 10 | 0.03 | 0.02 | 0.9718 |
| 3 | 33 | 34 | 0.02 | 0.01 | 0.9971 |
| 4 | 48 | 49 | 0.38 | 0.27 | 0.9944 |
| 5 | 49 | 50 | 0.38 | 0.27 | 0.9937 |

5. Conclusions

For finding the MLM and PLM, unique and innovative formulae considering line resistance are so developed that they can be applied for both the transmission and distribution systems. These formulae can be effectively applied to both transmission and distribution systems. This research paper focuses on the 57-bus test system for transmission and the 69-bus test system for distribution. MLM gives the VCP, or maximum loadability limit, which is useful for voltage stability analysis. On the other hand, it is essential to ensure the safe, reliable, and practical operation of the power system by maintaining the voltage magnitude above the lower limit of voltage constraints limit (i.e., 0.9–1.1 p.u.). In light of the idea, an efficient and logical formula for PLM is developed to calculate the maximum practical permitted load for a particular bus. To justify the results of the newly proposed simple formulae, a comparison is done between the results obtained from the NRLF and CLF methods and the result obtained from the proposed non-iterative formula-based techniques. To compare the simulation time, a comparison of estimated time is also performed to showcase the effectiveness of the proposed formula. From the results, it can be concluded that the developed formulae are very effective and fruitful for planning engineers to decide about new connections, additional load demand by the existing consumers, or the optimum capacity of an EV charging station for a bus, and also it takes less time as compared to the conventional method to get the result. The application of EV fast charging stations is also implemented for both 57-bus and 69-bus test systems to prove the efficacy of the proposed method.

Author Contributions: Conceptualization, S.N., S.R.G. and P.A.; methodology, S.N., S.R.G. and P.A.; software, S.N.; validation, S.N., S.R.G., P.A. and F.L.; formal analysis, S.N., S.R.G., P.A. and F.L.; investigation, S.N., S.R.G., P.A. and F.L.; writing—original draft preparation, S.N. and P.A.; supervision, S.R.G., P.A. and F.L.; project administration, S.R.G. and P.A. All authors have read and agreed to the published version of the manuscript.

Funding: This research received no external funding.

Data Availability Statement: Data related to the 57-bus interconnected system and 69-bus radial distribution system used in this work is available in [32–35].

Acknowledgments: We are extremely grateful to the School of Electrical Engineering, KIIT deemed to be University, Bhubaneswar for their continual support and inspiration in ensuring the completion of the research work.

Conflicts of Interest: The authors declare no conflict of interest.

Appendix A. Derivation of MLM

Considering both the resistance and reactance of the line, the formulations of power balance are shown below.

$$I_{12} = \frac{S^*}{V^*} = \frac{P_2 - jQ_2}{V_2 \angle -\delta_2} \quad (A1)$$

$$V_1 \angle \delta_1 = V_2 \angle \delta_2 + I_{12}(R_{12} + jX_{12})$$

$$\text{Or, } V_1 \angle \delta_1 = V_2 \angle \delta_2 + \frac{P_2 - jQ_2}{V_2 \angle -\delta_2} (R_{12} + jX_{12}) \quad [\text{using (A1)}]$$

$$\text{Or, } V_1 \angle \delta_1 = \frac{|V_2|^2 + P_2 R_{12} + Q_2 X_{12} + j(P_2 X_{12} - Q_2 R_{12})}{V_2 \angle -\delta_2}$$

$$\text{Or, } V_1 V_2 \angle \delta_1 - \delta_2 = \left(|V_2|^2 + P_2 R_{12} + Q_2 X_{12} \right) + j(P_2 X_{12} - Q_2 R_{12}) \quad (A2)$$

Taking the Mod value on both sides of (A2), we get

$$|V_1|^2 |V_2|^2 = \left(|V_2|^2 + P_2 R_{12} + Q_2 X_{12} \right)^2 + (P_2 X_{12} - Q_2 R_{12})^2$$

$$\text{Or, } |V_1|^2 |V_2|^2 = |V_2|^4 + 2|V_2|^2 (P_2 R_{12} + Q_2 X_{12}) + (P_2 R_{12} + Q_2 X_{12})^2 + (P_2 X_{12} - Q_2 R_{12})^2$$

$$\text{Or, } 0 = |V_2|^4 + 2|V_2|^2 (P_2 R_{12} + Q_2 X_{12}) + (P_2 R_{12} + Q_2 X_{12})^2 + (P_2 X_{12} - Q_2 R_{12})^2 - |V_1|^2 |V_2|^2$$

$$\text{Or, } \left(|V_2|^2 \right)^2 + |V_2|^2 \left[2(P_2 R_{12} + Q_2 X_{12}) - |V_1|^2 \right] + (P_2 R_{12} + Q_2 X_{12})^2 + (P_2 X_{12} - Q_2 R_{12})^2 = 0 \quad (A3)$$

Equation (A3) can be expressed as a quadratic equation like (A4),

$$ax^2 + bx + c = 0 \quad (A4)$$

Comparing the (A3) and (A4), we have

$$x = |V_2|^2$$

$$a = 1$$

$$b = 2(P_2 R_{12} + Q_2 X_{12}) - |V_1|^2$$

$$c = (P_2 R_{12} + Q_2 X_{12})^2 + (P_2 X_{12} - Q_2 R_{12})^2$$

Here x never be negative or imaginary. For getting real and positive roots, the following condition must be satisfied.

$$b^2 - 4ac \geq 0 \quad (\text{A5})$$

Putting the value of a , b , and c into (A5), we get

$$\left[2(P_2 R_{12} + Q_2 X_{12}) - |V_1|^2 \right]^2 - 4 * 1 * \left[(P_2 R_{12} + Q_2 X_{12})^2 + (P_2 X_{12} - Q_2 R_{12})^2 \right] \geq 0$$

$$\text{Or, } 4(P_2 R_{12} + Q_2 X_{12})^2 - 4(P_2 R_{12} + Q_2 X_{12})|V_1|^2 + |V_1|^4 - 4 * 1 * \left[(P_2 X_{12} - Q_2 R_{12})^2 + (P_2 R_{12} + Q_2 X_{12})^2 \right] \geq 0$$

$$\text{Or, } 4(P_2 R_{12} + Q_2 X_{12})^2 - 4(P_2 R_{12} + Q_2 X_{12})|V_1|^2 + |V_1|^4 - 4(P_2 X_{12} - Q_2 R_{12})^2 - 4(P_2 R_{12} + Q_2 X_{12})^2 \geq 0$$

$$\text{Or, } |V_1|^4 - 4(P_2 R_{12} + Q_2 X_{12})|V_1|^2 - 4(P_2 X_{12} - Q_2 R_{12})^2 \geq 0$$

$$\text{Or, } |V_1|^4 + [-4(P_2 R_{12} + Q_2 X_{12})]|V_1|^2 + [-4(P_2 X_{12} - Q_2 R_{12})^2] \geq 0 \quad (\text{A6})$$

In the voltage stability analysis such as the PV curve, the load increases gradually using a load multiplier, keeping the power factor constant. In other words, load ($P_L + Q_L$) is multiplied by the same multiplier. The value of the MLM gives the information about how much load ($P + jQ$) can be increased so that the system will remain in a stable condition. The MLM is multiplied by the load of the receiving end bus (REB) i.e., $P' = P * MLM$ and $Q' = Q * MLM$. Therefore, $(P' + jQ') = (P + jQ) * MLM$. Now, (A6) can be formulated as

$$|V_1|^4 + [-4(P_2 R_{12} + Q_2 X_{12})] * MLM * |V_1|^2 + [-4(P_2 X_{12} - Q_2 R_{12})^2] * MLM^2 = 0$$

$$\text{Or, } \left[4(P_2 X_{12} - Q_2 R_{12})^2 \right] * LM^2 + 4(P_2 R_{12} + Q_2 X_{12}) * |V_1|^2 * LM - |V_1|^4 = 0$$

The above equation can be re-written as

$$a * MLM^2 + b * MLM + c = 0$$

where,

$$4 * (P_2 X_{12} - Q_2 R_{12})^2 = a$$

$$4 * (P_2 R_{12} + Q_2 X_{12}) * |V_1|^2 = b$$

$$(-|V_1|^4) = c$$

The value of MLM is determined as follows:

$$MLM = \frac{-b \pm \sqrt{(b^2 - 4ac)}}{2a}$$

As the MLM is always positive, the MLM is given below:

$$MLM = \frac{\sqrt{(b^2 - 4ac)}}{2a} - \frac{b}{2a} \quad (\text{A7})$$

General equation of MLM:

Put the values of a, b, and c in (A7), and we get

$$MLM = \frac{\sqrt{\left[16(P_2R_{12} + Q_2X_{12})^2 * |V_1|^4 - 4 * 4(P_2X_{12} - Q_2R_{12})^2 * (-|V_1|^4)\right]}}{2 * 4(P_2X_{12} - Q_2R_{12})^2} - \frac{4(P_2R_{12} + Q_2X_{12}) * |V_1|^2}{2 * 4(P_2X_{12} - Q_2R_{12})^2}$$

$$\text{Or, } MLM = \frac{\sqrt{\left[16(P_2R_{12} + Q_2X_{12})^2 * |V_1|^4 + 16 * (P_2X_{12} - Q_2R_{12})^2 * (|V_1|^4)\right]}}{8 * (P_2X_{12} - Q_2R_{12})^2} - \frac{4(P_2R_{12} + Q_2X_{12}) * |V_1|^2}{8 * (P_2X_{12} - Q_2R_{12})^2}$$

$$MLM = \frac{|V_1|^2}{2(P_2X_{12} - Q_2R_{12})^2} \left\{ \sqrt{\left[(P_2R_{12} + Q_2X_{12})^2 + (P_2X_{12} - Q_2R_{12})^2\right]} - (P_2R_{12} + Q_2X_{12}) \right\} \quad (A8)$$

Appendix B. Derivation of PLM

Considering the practical constraints, the PLM is determined as follows:

Putting $V_2 = 0.9$ in (A3), we get

$$(0.9)^4 + (0.9)^2 \left[2(P_2R_{12} + Q_2X_{12}) * PLM - |V_1|^2 \right] + (P_2R_{12} + Q_2X_{12})^2 * PLM^2 + (P_2X_{12} - Q_2R_{12})^2 * PLM^2 = 0 \quad (A9)$$

$$\text{Or, } (0.9)^4 + (0.9)^2 * 2(P_2R_{12} + Q_2X_{12}) * PLM - |V_1|^2 * (0.9)^2 + \left[(P_2R_{12} + Q_2X_{12})^2 + (P_2X_{12} - Q_2R_{12})^2 \right] * PLM^2 = 0 \quad (A10)$$

Arranging (A10) in the form of a quadratic equation,

$$\left[(P_2R_{12} + Q_2X_{12})^2 + (P_2X_{12} - Q_2R_{12})^2 \right] * PLM^2 + (0.9)^2 * 2(P_2R_{12} + Q_2X_{12}) * PLM + \left[(0.9)^4 - |V_1|^2 * (0.9)^2 \right] = 0 \quad (A11)$$

where,

$$(P_2R_{12} + Q_2X_{12})^2 + (P_2X_{12} - Q_2R_{12})^2 = a$$

$$(0.9)^2 * 2(P_2R_{12} + Q_2X_{12}) = b$$

$$(0.9)^4 - |V_1|^2 * (0.9)^2 = c$$

Again,

$$PLM = \frac{\sqrt{(b^2 - 4ac)}}{2a} - \frac{b}{2a}$$

Put the values of a, b, and c

$$PLM = \frac{\sqrt{\left[\left\{ 4 * (0.9)^4 * (P_2R_{12} + Q_2X_{12})^2 \right\} - 4 * \left\{ (P_2R_{12} + Q_2X_{12})^2 + (P_2X_{12} - Q_2R_{12})^2 \right\} * \left\{ (0.9)^4 - |V_1|^2 * (0.9)^2 \right\} \right]}}{2 * \left\{ (P_2R_{12} + Q_2X_{12})^2 + (P_2X_{12} - Q_2R_{12})^2 \right\}} - \frac{(0.9)^2 * 2(P_2R_{12} + Q_2X_{12})}{2 * \left\{ (P_2R_{12} + Q_2X_{12})^2 + (P_2X_{12} - Q_2R_{12})^2 \right\}} \quad (A12)$$

References

1. Prudenzi, A.; Silvestri, A.; Lucci, G.; Regoli, M. Analysis of Residential Standby Power Demand Control through a Psychological Model of Demand. In Proceedings of the 10th International Conference on Environment and Electrical Engineering, Rome, Italy, 8–11 May 2011.
2. Tang, X.; Milanovic, J.V. Assessment of the Impact of Demand Side Management on Power System Small Signal Stability. In Proceedings of the IEEE Manchester Power Tech, Manchester, UK, 18–22 June 2017.
3. Tusciano, A.A.; Gabhane, S.K. A Method for Optimal Usage of Power in Electric Vehicle. In Proceedings of the International Conference on Inventive Computation Technologies (ICICT), Coimbatore, India, 26–27 August 2016.
4. Joshi, A.; Sharma, R.; Baral, B. Comparative Life Cycle Assessment of Conventional Combustion Engine Vehicle, Battery Electric Vehicle and Fuel Cell Electric Vehicle in Nepal. *J. Clean. Prod.* **2022**, *379*, 134407. [\[CrossRef\]](#)
5. Mastoi, M.S.; Zhuang, S.; Munir, H.M.; Haris, M.; Hassan, M.; Usman, M.; Bukhari, S.S.H.; Ro, J.-S. An In-Depth Analysis of Electric Vehicle Charging Station Infrastructure, Policy Implications, and Future Trends. *Energy Rep.* **2022**, *8*, 11504–11529. [\[CrossRef\]](#)
6. Nafi, I.M.; Tabassum, S.; Hassan, Q.R.; Abid, F. Effect of Electric Vehicle Fast Charging Station on Residential Distribution Network in Bangladesh. In Proceedings of the 5th International Conference on Electrical Engineering and Information Communication Technology (ICEEICT), Dhaka, Bangladesh, 18–20 November 2021.
7. Nutkani, I.U.; Lee, J.C. Evaluation of Electric Vehicles (EVs) Impact on Electric Grid. In Proceedings of the International Power Electronics Conference (IPEC-Himeji 2022-ECCE Asia), Himeji, Japan, 15–19 May 2022.
8. Savari, G.F.; Sathik, M.J.; Raman, L.A.; El-Shahat, A.; Hasanien, H.M.; Almakhlles, D.; Abdel Aleem, S.H.E.; Omar, A.I. Assessment of Charging Technologies, Infrastructure and Charging Station Recommendation Schemes of Electric Vehicles: A Review. *Ain Shams Eng. J.* **2023**, *14*, 101938. [\[CrossRef\]](#)
9. Olcay, K.; Çetinkaya, N. Analysis of the Electric Vehicle Charging Stations Effects on the Electricity Network with Artificial Neural Network. *Energies* **2023**, *16*, 1282. [\[CrossRef\]](#)
10. Adebayo, I.G.; Sun, Y. Performance Evaluation of Voltage Stability Indices for a Static Voltage Collapse Prediction. In Proceedings of the IEEE PES/IAS PowerAfrica, Nairobi, Kenya, 25–28 August 2020.
11. Bento, M.E.C. A Method for Monitoring the Load Margin of Power Systems under Load Growth Variations. *Sustain. Energy Grids Netw.* **2022**, *30*, 100677. [\[CrossRef\]](#)
12. Adetokun, B.B.; Muriithi, C.M.; Ojo, J.O. Voltage Stability Assessment and Enhancement of Power Grid with Increasing Wind Energy Penetration. *Int. J. Electr. Power Energy Syst.* **2020**, *120*, 105988. [\[CrossRef\]](#)
13. Mallick, S.; Acharjee, P.; Ghoshal, S.P.; Thakur, S.S. Determination of Maximum Load Margin Using Fuzzy Logic. *Int. J. Electr. Power Energy Syst.* **2013**, *52*, 231–246. [\[CrossRef\]](#)
14. Bonini Neto, A.; Alves, D.A.; Minussi, C.R. Artificial Neural Networks: Multilayer Perceptron and Radial Basis to Obtain Post-Contingency Loading Margin in Electrical Power Systems. *Energies* **2022**, *15*, 7939. [\[CrossRef\]](#)
15. Mishra, S.; Brar, Y.S. Load Flow Analysis Using MATLAB. In Proceedings of the IEEE International Students' Conference on Electrical, Electronics and Computer Science (SCEECS), Bhopal, India, 19–20 February 2022.
16. Chatterjee, S.; Mandal, S. A Novel Comparison of Gauss-Seidel and Newton-Raphson Methods for Load Flow Analysis. In Proceedings of the International Conference on Power and Embedded Drive Control (ICPEDC), Chennai, India, 16–18 March 2017.
17. Ajarapu, V.; Christy, C. The Continuation Power Flow: A Tool for Steady State Voltage Stability Analysis. *IEEE Trans. Power Syst.* **1992**, *7*, 416–423. [\[CrossRef\]](#)
18. Lou, Y.; Ou, Z.; Tong, Z.; Tang, W.; Li, Z.; Yang, K. Static Voltage Stability Evaluation on the Urban Power System by Continuation Power Flow. In Proceedings of the 5th International Conference on Energy, Electrical and Power Engineering (CEEPE), Chongqing, China, 22–24 April 2022.
19. Jmii, H.; Meddeb, A.; Chebbi, S. Newton-Raphson Load Flow Method for Voltage Contingency Ranking. In Proceedings of the 15th International Multi-Conference on Systems, Signals & Devices (SSD), Hammamet, Tunisia, 19–22 March 2018.
20. Thiyagarajan, T.; Mv, S.; Samy, A.K.; Venkadesan, A. Performance Investigation of SVR for Evaluating Voltage Stability Margin in a Power Utility. In Proceedings of the IEEE International Power and Renewable Energy Conference (IPRECON), Kollam, India, 24–26 September 2021.
21. Montoya, O.D.; Gil-Gonzalez, W.; Garrido, V.M. Voltage Stability Margin in DC Grids with CPLs: A Recursive Newton-Raphson Approximation. *IEEE Trans. Circuits Syst. II* **2020**, *67*, 300–304. [\[CrossRef\]](#)
22. Roy Ghatak, S.; Sannigrahi, S.; Acharjee, P. Comparative Performance Analysis of DG and DSTATCOM Using Improved PSO Based on Success Rate for Deregulated Environment. *IEEE Syst. J.* **2018**, *12*, 2791–2802. [\[CrossRef\]](#)
23. Modarresi, J.; Gholipour, E.; Khodabakhshian, A. A Comprehensive Review of the Voltage Stability Indices. *Renew. Sustain. Energy Rev.* **2016**, *63*, 1–12. [\[CrossRef\]](#)
24. Mokred, S.; Wang, Y.; Chen, T. Modern Voltage Stability Index for Prediction of Voltage Collapse and Estimation of Maximum Load-Ability for Weak Buses and Critical Lines Identification. *Int. J. Electr. Power Energy Syst.* **2023**, *145*, 108596. [\[CrossRef\]](#)
25. Kayal, P.; Chanda, C.K. Placement of Wind and Solar Based DGs in Distribution System for Power Loss Minimization and Voltage Stability Improvement. *Int. J. Electr. Power Energy Syst.* **2013**, *53*, 795–809. [\[CrossRef\]](#)
26. Danish, M.S.S.; Senjyu, T.; Danish, S.M.S.; Sabory, N.R.; K, N.; Mandal, P. A Recap of Voltage Stability Indices in the Past Three Decades. *Energies* **2019**, *12*, 1544. [\[CrossRef\]](#)

27. Musirin, I.; Abdul Rahman, T.K. Novel Fast Voltage Stability Index (FVSI) for Voltage Stability Analysis in Power Transmission System. In Proceedings of the Student Conference on Research and Development, Shah Alam, Malaysia, 16–17 July 2002.
28. Meena, M.K.; Kumar, N. On-Line Monitoring and Simulation of Transmission Line Network Voltage Stability Using FVSI. In Proceedings of the 2nd IEEE International Conference on Power Electronics, Intelligent Control and Energy Systems (ICPEICES), Delhi, India, 22–24 October 2018.
29. Samuel, I.A.; Soyemi, A.O.; Awelewa, A.A.; Olajube, A.A.; Ketande, J. Review of Voltage Stability Indices. *IOP Conf. Ser. Earth Environ. Sci.* **2021**, *730*, 012024. [\[CrossRef\]](#)
30. Yari, S.; Khoshkhoo, H. Assessment of Line Stability Indices in Detection of Voltage Stability Status. In Proceedings of the IEEE International Conference on Environment and Electrical Engineering and 2017 IEEE Industrial and Commercial Power Systems Europe (EEEIC/I&CPS Europe), Milan, Italy, 6–9 June 2017.
31. Okon, T.; Wilkosz, K. A Simple Contingency Selection for Voltage Stability Analysis. *ElAEE* **2013**, *19*, 25–28. [\[CrossRef\]](#)
32. Gautam, M.; Bhusal, N.; Thapa, J.; Benidris, M. A Cooperative Game Theory-Based Approach to Formulation of Distributed Slack Buses. *Sustain. Energy Grids Netw.* **2022**, *32*, 100890. [\[CrossRef\]](#)
33. Power Systems Test Case Archive. University of Washington. Available online: <https://labs.ece.uw.edu/pstca/> (accessed on 30 May 2023).
34. Azam Muhammad, M.; Mokhlis, H.; Naidu, K.; Amin, A.; Fredy Franco, J.; Othman, M. Distribution Network Planning Enhancement via Network Reconfiguration and DGIntegration Using Dataset Approach and Water Cycle Algorithm. *J. Mod. Power Syst. Clean Energy* **2020**, *8*, 86–93. [\[CrossRef\]](#)
35. Sarwar, S.; Mokhlis, H.; Othman, M.; Muhammad, M.A.; Laghari, J.A.; Mansor, N.N.; Mohamad, H.; Pourdayaei, A. A Mixed Integer Linear Programming Based Load Shedding Technique for Improving the Sustainability of Islanded Distribution Systems. *Sustainability* **2020**, *12*, 6234. [\[CrossRef\]](#)
36. Guerriche, K.R.; Bouktir, T. Maximum Loading Point in Distribution System with Renewable Resources Penetration. In Proceedings of the International Renewable and Sustainable Energy Conference (IRSEC), Ouarzazate, Morocco, 17–19 October 2014.
37. Choudekar, P.; Sinha, S.K.; Siddiqui, A. Optimal Location of SVC for Improvement in Voltage Stability of a Power System under Normal and Contingency Condition. *Int. J. Syst. Assur. Eng. Manag.* **2017**, *8*, 1312–1318. [\[CrossRef\]](#)

Disclaimer/Publisher’s Note: The statements, opinions and data contained in all publications are solely those of the individual author(s) and contributor(s) and not of MDPI and/or the editor(s). MDPI and/or the editor(s) disclaim responsibility for any injury to people or property resulting from any ideas, methods, instructions or products referred to in the content.